Available online at www.sciencedirect.com
ScienceDirect
Journal of Solid State Chemistry 179 (2006) 3461–3466
Journal of Solid State Chemistry
www.elsevier.com/locate/jssc

Synthesis, structure and magnetic properties of new phosphates $K_2Mn_{0.5}Ti_{1.5}(PO_4)_3$ and $K_2Co_{0.5}Ti_{1.5}(PO_4)_3$ with the langbeinite structure

Ivan V. Ogorodnyk[a,*], Igor V. Zatovsky[a], Nikolay S. Slobodyanik[a], Vyacheslav N. Baumer[b], Oleg V. Shishkin[b]

[a]*Department of Inorganic Chemistry, Taras Shevchenko National University, Volodymyrska str. 64, Kyiv 01033, Ukraine*
[b]*STC "Institute for Single Crystals", National Academy of Science of Ukraine, Lenina ave. 60, Kharkiv 61001, Ukraine*

Received 31 January 2006; received in revised form 3 April 2006; accepted 12 July 2006
Available online 16 July 2006

Abstract

New complex phosphates of the general formula $K_2M_{0.5}Ti_{1.5}(PO_4)_3$ ($M =$ Mn, Co) have been obtained from the melting mixture of KPO_3, $K_4P_2O_7$, TiO_2 and $CoCO_3 \cdot mCo(OH)_2$ or $Mn(H_2PO_4)_2$ by means of a flux technique. The synthesized phosphates have been characterized by the single-crystal X-ray diffraction and the FTIR-spectroscopy. The compounds crystallize in the cubic system with the space group $P2_13$ and cell parameters $a = 9.9030(14)$ Å for $K_2Mn_{0.5}Ti_{1.5}(PO_4)_3$ and $a = 9.8445(12)$ Å for $K_2Co_{0.5}Ti_{1.5}(PO_4)_3$. Both phosphates are isostructural with the langbeinite mineral and contain four formula unit $K_2M_{0.5}Ti_{1.5}(PO_4)_3$ per unit cell. The structure can be described using $[M_2(PO_4)_3]$ framework composed of two $[MO_6]$ octahedra interlinked via three $[PO_4]$ tetrahedra. The Curie–Weiss-type behavior is observed in the magnetic susceptibility.

Keywords: Phosphates; Crystal structure; Single-crystal X-ray diffraction; $K_2M_{0.5}Ti_{1.5}(PO_4)_3$; Langbeinite; FTIR spectra; Magnetic measurements

1. Introduction

There are several possibilities of structure formation towards the compounds containing the $[M_2(XO_4)_3]$ fragment into framework. They are common structural types of garnet, nasicon, alluaudite, $Sc_2(WO_4)_3$ and langbeinite. In general, these structures have the same type of framework and different types of holes, cavities, tunnels for accommodation cations. Physical and chemical properties of all these types of compounds depend on their structure.

The langbeinite-type compounds have general formula $Cat_{2-X}M_2(XO_4)_3$ ($x \leqslant 1$; Cat-alkaline metals, Tl, NH_4, Ca, Sr, Ba; $M =$ transition metal; $X =$ S, P, As, Si, V, etc.), and crystallize in a cubic phase (space group $P2_13$). A feature of such compounds are 3D-framework built up from metal octahedra and anionic tetrahedra which are linked via vertexes and big closed interstitial holes which can be filled up by large mono- or divalent cations.

Nowadays there are a number of reports on synthesis and investigation of langbeinite-like compounds. Among them, the most interesting works are on langbeinites where network is formed from polyhedra of three (Ti, Fe, Cr, V, Y, rare-earth elements) or tetra valent (Ti, Zr) metals, while the interstitial cations are Na, K, Ba: $KTi_2(PO_4)_3$ [1], $K_2Ti_2(PO_4)_3$ [2–4], $K_{1.388}Ti_{1.885}Al_{0.115}(PO_4)_3$ [5], $K_2MZr(PO_4)_3$ ($M =$ Y, Gd) [6], $K_2FeZr(PO_4)_3$ [7], $Na_2MTi(PO_4)_3$ ($M =$ Fe, Cr) [8], $K_2MTi(PO_4)_3$ ($M =$ Er, Yb, Y, Cr) [9], $K_2BiHf(PO_4)_3$ [10], $Ba_{1.5}V_2(PO_4)_3$ [11], etc.

The langbeinite-like compounds can be proposed as new magnetic and luminescence materials. Luminescence and magnetic properties depend on the nature of the ions which form compound. For example, including of the paramagnetic transition ions into the compound makes possible realization of the exchange interactions in the M–O–P–O–M chains because the distance between paramagnetic centers is in the range of 4.5–5.0 Å.

---

[*] Corresponding author.
E-mail address: ogorod@bigmir.net (I.V. Ogorodnyk).

0022-4596/$ - see front matter © 2006 Elsevier Inc. All rights reserved.
doi:10.1016/j.jssc.2006.07.015

Herein, we report a new type of langbeinite-related compounds which consisted di- and tetra-valent cations. We investigate formation of the langbeinites with general formula $K_2M_{0.5}Ti_{1.5}(PO_4)_3$, where $M = $ Mn, Co. Synthesis, structural characterization and magnetic measurements of titled compounds are discussed here.

2. Experimental

2.1. Synthesis

Dark brown crystals of the title compounds have been prepared by the flux technique. As initial reagents, KPO_3 (pure), $K_4P_2O_7$ (pure), TiO_2 (extra pure), $CoCO_3 \cdot mCo(OH)_2$ (68.26% CoO mass, analytical grade), $Mn(H_2PO_4)_2 \cdot 2H_2O$ (prepared according to Kopilevitch et al. [12]) were used both for flux and crystals. Grounded mixtures of 4.87 g KPO_3, 4.93 g $K_4P_2O_7$, 1.220 g TiO_2, 4.35 g $Mn(H_2PO_4)_2 \cdot 2H_2O$ for $K_2Mn_{0.5}Ti_{1.5}(PO_4)_3$ and 12.0 g KPO_3, 1.017 g TiO_2 and 1.676 g $CoCO_3 \cdot mCo(OH)_2$ for $K_2Co_{0.5}Ti_{1.5}(PO_4)_3$ were placed into platinum crucibles. Crucibles were heated up to 1050 °C. The mixtures melt at this temperature to homogenous liquid. Then the melts were cooled down to 720 °C at a rate of 25 °C h^{-1} that afforded the crystalline products. Obtained crystals were separated from flux by washing with boiling water. Both compounds form crystals which have preferably tetrahedral habitus. The analysis of the elements K, Ti, Mn, Co and P was performed by energy dispersive spectroscopy using a Link Isis analyzer mounted on a Philips XL 30 FE 6 scanning electron microscope. The atomic ratio of the elements in the titled compounds was found to be 4:3:1:6 for K/Ti/M^{II}/P, respectively.

2.2. X-ray data collection and crystal data

For single crystal X-ray diffraction dark red tetrahedron-shaped crystal of $K_2Co_{0.5}Ti_{1.5}(PO_4)_3$ and dark brown polyhedron-shaped crystal of $K_2Mn_{0.5}Ti_{1.5}(PO_4)_3$ were selected. X-ray experiment was performed on Oxford-Diffraction XCalibur 3 diffractometer with 2048 × 2048K (4 MPixel) CCD detector using monochromated Mo$K\alpha$ radiation ($\lambda = 0.71073$ Å). Analytical absorption correction was applied to the obtained data. An experiment was performed at 273 K. Cell parameters and space group were determined for manganese phosphate by 420 reflections ($15^\circ < \theta < 20^\circ$) and for cobalt phosphate by 340 reflections ($15^\circ < \theta < 25^\circ$). Crystal data and experimental conditions for intensity measurements and refinement are shown in Table 1.

The structures were solved with direct method using SHELXS-86 [13]. Two manganese (cobalt) sites were located on three-fold axis and one phosphorus site was located in a general position. Refinement based on this structural hypothesis followed by calculation of Fourier-difference maps revealed that four oxygen atoms are located in general positions, and two potassium atoms in special positions. Occupancy factor for potassium atoms is 1. Refinement was performed anisotropically using SHELXL-97 [14]. Titanium atoms appear in the same positions as manganese (cobalt) atoms. The hypothesis assumes a partial occupancy of the 3d-metal positions by Mn (Co) and Ti atoms. The sum of the occupancy factor is 1 for this position. For independent unit the sum of occupancy of Ti1 + Ti2 is 1.5. The positional disorder of 3d-metals in their positions is present. Three linear variable restraints (SUMP) were used to restraint the sum of occupation factors and charge to obtain electroneutrality of the compounds. The occupancies of transition metal sites by titanium and manganese (cobalt) atoms are shown in Table 2. The result of the structural analysis is in agreement with the chemical analysis.

Further details of the crystal structure investigations can be obtained from the Fachinformationszentrum Karlsruhe, 76344 Eggenstein-Leopoldshafen, Germany (fax: + 49 7247-808-666; e-mail: crysdata@fiz-karlsruhe.de) on quoting the depository number CSD-416204 for $K_2Mn_{0.5}Ti_{1.5}(PO_4)_3$ and CSD-416203 for $K_2Co_{0.5}Ti_{1.5}(PO_4)_3$.

2.3. Physical characterization

The FTIR-spectra recorded at room temperature in KBr disks using Nicolet Nexus FTIR spectrometer at 400–4000 cm^{-1}.

The powder X-ray diffraction (DRON-3 with monochromatized Cu$K\alpha_1$ radiation $\lambda = 1.54056$) confirmed that the obtained polycrystalline samples of $K_2Mn_{0.5}Ti_{1.5}(PO_4)_3$ and $K_2Co_{0.5}Ti_{1.5}(PO_4)_3$ were well crystallized and single phased. The X-ray powder diffraction patterns of the powder samples coincide with the generated from the single-crystal structural data. The impurities were not detected by the powder XRD.

The magnetic susceptibility was measured using Quantum Design Squid MPMS-XL magnetometer. The temperature and field dependence of the susceptibility of the container had been previously determined and their effect on the total susceptibility was negligible. The measurements were performed at 5.0 T over the 1.9–300 K temperature range. Magnetic susceptibility data for $K_2Mn_{0.5}Ti_{1.5}(PO_4)_3$ and $K_2Co_{0.5}Ti_{1.5}(PO_4)_3$ were acquired from the microcrystalline samples.

3. Results and discussion

3.1. Crystal structure

Final atomic coordinates and equivalent isotropic thermal parameters are shown in Table 2, and selected interatomic distances and bond angles are shown in Table 3.

The investigated compounds are isostructural to langbeinite $K_2Mg_2(SO_4)_3$ [15]. The structure of reported phosphates consists of [MeO_6] octahedra and [PO_4]

Table 1
Crystal data and refinement of $K_2Mn_{0.5}Ti_{1.5}(PO_4)_3$ and $K_2Co_{0.5}Ti_{1.5}(PO_4)_3$

	$K_2Mn_{0.5}Ti_{1.5}(PO_4)_3$	$K_2Co_{0.5}Ti_{1.5}(PO_4)_3$
Crystal data		
Crystal system	Cubic	Cubic
Space group	$P2_13$	$P2_13$
Cell parameter (Å)	9.9030(14)	9.8445(12)
V (Å^3)	971.2(2)	954.1(2)
Z	4	4
$\rho_{calc.}$ (g/cm^3)	3.162	3.233
Crystal dimensions (mm)	0.18 × 0.15 × 0.12	0.15 × 0.1 × 0.1
Data collection		
Measurement device	XCalibur 3 CCD	XCalibur 3 CCD
Wavelength (Å)	0.71073	0.71073
Monochromator	Graphite	Graphite
Scan mode	φ and ω	φ and ω
μ (mm^{-1})	3.303	3.57
Absorption correction	Analytical	Analytical
T_{min}, T_{max}	0.7249, 0.7821	0.6212, 0.7087
Number of reflections	18,683	18,203
Independent reflections	957	931
Reflections with $>2\sigma(I)$	956	927
$R_{int.}$	0.0391	0.0277
Theta max. (°)	29.99	29.84
$h=$, $k=$, $l=$	$-13\rightarrow13$; $-13\rightarrow13$; $-12\rightarrow13$	$-13\rightarrow13$; $-13\rightarrow11$; $-13\rightarrow13$
$F(000)$	898	902
Solution and refinement		
Primary solution method	Direct	Direct
Weighting scheme	$w = 1/[\sigma^2(F_o^2) + (0.0237P)^2 + 0.7806P]$, where $P = (F_o^2 + 2F_c^2)/3$	$w = 1/[\sigma^2(F_o^2) + (0.0363P)^2 + 1.3036P]$, where $P = (F_o^2 + 2F_c^2)/3$
R_1(all)	0.0205	0.0243
wR_2	0.05	0.0677
S	1.172	1.229
Number of parameters	62	62
Extinction correction	None	None
$(\Delta\rho)_{max,\ min}$ (e Å^{-3})	0.309, −0.295	0.409, −1.047
Flack parameter	−0.02(3)	0.02(3)

Table 2
Atomic coordinates and U_{eq} for $K_2Mn_{0.5}Ti_{1.5}(PO_4)_3$ and $K_2Co_{0.5}Ti_{1.5}(PO_4)_3$ in $P2_13$

Atom	Site	Occ.	x	y	z	Ueq
$K_2Mn_{0.5}Ti_{1.5}(PO_4)_3$						
Ti1/Mn1	4a	0.6992(9)/0.3008(9)	0.58545(4)	0.58545(4)	0.58545(4)	0.01038(13)
Ti2/Mn2	4a	0.8008(9)/0.1992(9)	0.85656(4)	0.85656(4)	0.85656(4)	0.01011(13)
K1	4a	1	0.06876(6)	0.06876(6)	0.06876(6)	0.0271(2)
K2	4a	1	0.29293(7)	0.29293(7)	0.29293(7)	0.0325(2)
P1	12b	1	0.62557(6)	0.45830(5)	0.27021(5)	0.01085(11)
O1	12b	1	0.6495(2)	0.5037(2)	0.4155(2)	0.0298(4)
O2	12b	1	0.7553(2)	0.4801(2)	0.1914(3)	0.0367(6)
O3	12b	1	0.58037(19)	0.31020(18)	0.2661(2)	0.0232(4)
O4	12b	1	0.5177(2)	0.5446(2)	0.2023(2)	0.0304(4)
$K_2Co_{0.5}Ti_{1.5}(PO_4)_3$						
Ti1/Co1	4a	0.7397(9)/0.2603(9)	0.89220(5)	0.89220(5)	0.89220(5)	0.00974(16)
Ti2/Co2	4a	0.7603(9)/0.2396(9)	0.16378(4)	0.16378(4)	0.16378(4)	0.00895(16)
K1	4a	1	0.68122(8)	0.68122(8)	0.68122(8)	0.0303(3)
K2	4a	1	0.45828(9)	0.45828(9)	0.45828(9)	0.0323(3)
P1	12b	1	0.47812(7)	0.29285(6)	0.12377(7)	0.00798(14)
O1	12b	1	0.5472(2)	0.2041(3)	0.2303(2)	0.0205(4)
O2	12b	1	0.4848(2)	0.4412(2)	0.1700(2)	0.0169(4)
O3	12b	1	0.3310(2)	0.2491(2)	0.1022(2)	0.0194(4)
O4	12b	1	0.2292(3)	0.0084(2)	0.0552(3)	0.0228(5)

Table 3
Selected bond distances (Å) and angles (deg) for $K_2Mn_{0.5}Ti_{1.5}(PO_4)_3$ and $K_2Co_{0.5}Ti_{1.5}(PO_4)_3$

$K_2Mn_{0.5}Ti_{1.5}(PO_4)_3$			
Ti1/Mn1–O1	1.972 (2) × 3	O1–Ti1/Mn1–O2	83.00 (8) × 3
Ti1/Mn1–O2	2.002 (2) × 3	O2–Ti1/Mn1–O2	90.72 (9) × 3
		O1–Ti1/Mn1–O1	93.22 (8) × 3
Ti2/Mn2–O3	1.980 (2) × 3	O1–Ti1/Mn1–O2	93.48 (10) × 3
Ti2/Mn2–O4	1.961 (2) × 3	O1–Ti1/Mn1–O2	172.48 (9) × 3
P1–O1	1.526 (2)	O3–Ti2/Mn2–O4	87.87(8) × 3
P1–O2	1.519 (2)	O4–Ti2/Mn2–O4	89.09 (8) × 3
P1–O3	1.534 (2)	O3–Ti2/Mn2–O4	91.44 (8) × 3
P1–O4	1.524 (2)	O3–Ti2/Mn2–O3	91.63 (8) × 3
		O3–Ti2/Mn2–O4	176.90 (8) × 3
K1–O1	2.868 (2) × 3		
K1–O4	2.953 (2) × 3	O2–P1–O4	106.64 (11)
K1–O2	3.074 (3) × 3	O2–P1–O1	108.14 (14)
K1–O2	3.207 (3) × 3	O4–P1–O3	108.65 (11)
		O3–P1–O1	110.61 (11)
K2–O3	2.864 (2) × 3	O4–P1–O1	111.08 (11)
K2–O4	3.093 (2) × 3	O3–P1–O2	111.66 (11)
K2–O2	3.138 (2) × 3		
K2–O4	3.460 (2) × 3		
$K_2Co_{0.5}Ti_{1.5}(PO_4)_3$			
Ti1/Co1–O1	1.948 (2) × 3	O1–Ti1/Co1–O1	88.42 (9) × 3
Ti1/Co1–O2	1.974 (2) × 3	O1–Ti1/Co1–O1	90.08 (10) × 3
		O1–Ti1/Co1–O2	90.52 (10) × 3
Ti2/Co2–O3	1.945 (2) × 3	O2–Ti1/Co1–O2	90.99 (8) × 3
Ti2/Co2–O4	1.974 (2) × 3	O1–Ti1/Co1–O2	178.39 (9) × 3
P1–O1	1.525 (2)	O3–Ti2/Co2–O4	83.67 (10) × 3
P1–O2	1.531 (2)	O4–Ti2/Co2–O4	90.57 (11) × 3
P1–O3	1.526 (2)	O3–Ti2/Co2–O3	91.89 (8) × 3
P1–O4	1.522 (2)	O3–Ti2/Co2–O4	94.35 (10) × 3
		O3–Ti2/Co2–O4	172.45 (9) × 3
K1–O3	2.872 (2) × 3		
K1–O1	2.942 (2) × 3	O1–P1–O4	106.49 (12)
K1–O4	3.015 (3) × 3	O3–P1–O4	108.30 (14)
K1–O4	3.231 (3) × 3	O1–P1–O2	108.84 (14)
		O2–P1–O3	110.57 (11)
K2–O2	2.855 (2) × 3	O1–P1–O3	110.93 (11)
K2–O1	3.051 (3) × 3	O2–P1–O4	111.64 (13)
K2–O4	3.119 (3) × 3		
K2–O1	3.473 (3) × 3		

tetrahedra which are linked via vertexes forming three-dimensional framework. The potassium cations are located in large closed cavities within the framework.

The {Me1–Me2–K1–K2} sequence runs along the direction [111]. Two independent octahedra on cubic cell diagonal are connected into pairs by three phosphate tetrahedra. Thus, the sequence of dual octahedra groups separated by two cation sites with symmetry 3 {$[Me1O_6]$–$[PO_4]_3$–$[Me2O_6]$–K1–K2} is formed (Fig. 1a). Each orthophosphate tetrahedra via two vertexes links a pair the octahedra of one sequence, and via two others joins two octahedra of two different sequences.

In both structures, the octahedral coordination environments of Co(II) and Mn(II) are slightly distorted as bond lengths Me–O and angles O–Me–O indicate. The Me–O bond ranges are 1.961(2)–2.002(2) and 1.945(2)–1.974(2) Å for $K_2Mn_{0.5}Ti_{1.5}(PO_4)_3$ and $K_2Co_{0.5}Ti_{1.5}(PO_4)_3$, respectively. Such length values are usual for Ti–O contact. In cubic polymorph of $KTi_2(PO_4)_3$ ($P2_13$) [1] Ti–O bonds range are 1.877(10)–1.965(10) Å. Me–O bond lengths in titled structures are slightly smaller, than the corresponding bond lengths in usual manganese and cobalt structures, but are close to those in $[CoO_6]$ polyhedra in $Co_3(PO_4)_2$ [16]. It could be explained by the small occupancy of cobalt and manganese sites. It should be noted that the occupancy of transition metal sites by cobalt atoms is near to 0.25 for both positions (Table 2), whereas in case of manganese it differs a lot (~0.3 for Mn1 site and ~0.2 for Mn2 site). This fact explains differences in environment of two transition metal positions in both structures. As shown in Table 3, the values of the bond lengths in octahedron of two Co sites are close to each other, but bond lengths of Mn1–O and Mn2–O differ a lot. Mn–O contacts for the Mn1 atom have longer distances than for the Mn2 atom.

P–O bond lengths for both structures are in a range of 1.519(2)–1.534(2) Å and 1.522(2)–1.531(2) Å for $K_2Mn_{0.5}Ti_{1.5}(PO_4)_3$ and $K_2Co_{0.5}Ti_{1.5}(PO_4)_3$, respectively. O–P–O angle values are close to tetrahedral. Comparing corresponding interatomic distances and bond angles for octahedra and tetrahedra, it is necessary to note that the coordination environment of the transition metal and phosphorus in manganese structure is more distorted than in cobalt structure.

Potassium atoms are found in 12 coordinated states. Four types of interatomic contacts K–O are observed as indicated in Table 3. Three contacts of each type are present in consideration with sites symmetry. Big cavity containing two potassium atoms is shown in Fig. 1b.

3.2. FTIR-spectra

The FTIR spectra of $K_2Mn_{0.5}Ti_{1.5}(PO_4)_3$ (1) and $K_2Co_{0.5}Ti_{1.5}(PO_4)_3$ (2) are shown in Fig. 2. The IR spectra of both titled compounds exhibit all the bands predicted by group theory. The $[PO_4]$ tetrahedron is somewhat distorted and has the local symmetry *C1*. The bands in the range 1200–850 cm^{-1} are due to the P–O stretching frequencies in the $[PO_4]$ tetrahedron: doublet 1189, 1161 for $K_2Mn_{0.5}Ti_{1.5}(PO_4)_3$ (1191, 1158 for $K_2Co_{0.5}Ti_{1.5}(PO_4)_3$); 1091 (1088); 1034 (1036); strong 996 (988); shoulder 967 (960); shoulder 912 (910); shoulder 863(858) cm^{-1}. The 670–540 region shows bonds bending vibrations of P–O: 648 (647); shoulder 630 (618); 578 (577); 546 (546) cm^{-1}. A group of bands in region 500–400 cm^{-1} can be attributed to M–O vibrations: triplet 475, 459, 449 (475, 461, 449) and shoulder 433 cm^{-1}.

The observed differences in FTIR spectra can be assumed with differences in local phosphorus and 3*d*-metal environment.

3.3. Magnetic properties

The temperature dependence of the reciprocal molar magnetic susceptibility for both compounds is shown in Fig. 3. $K_2Mn_{0.5}Ti_{1.5}(PO_4)_3$ displays a Curie–Weiss law

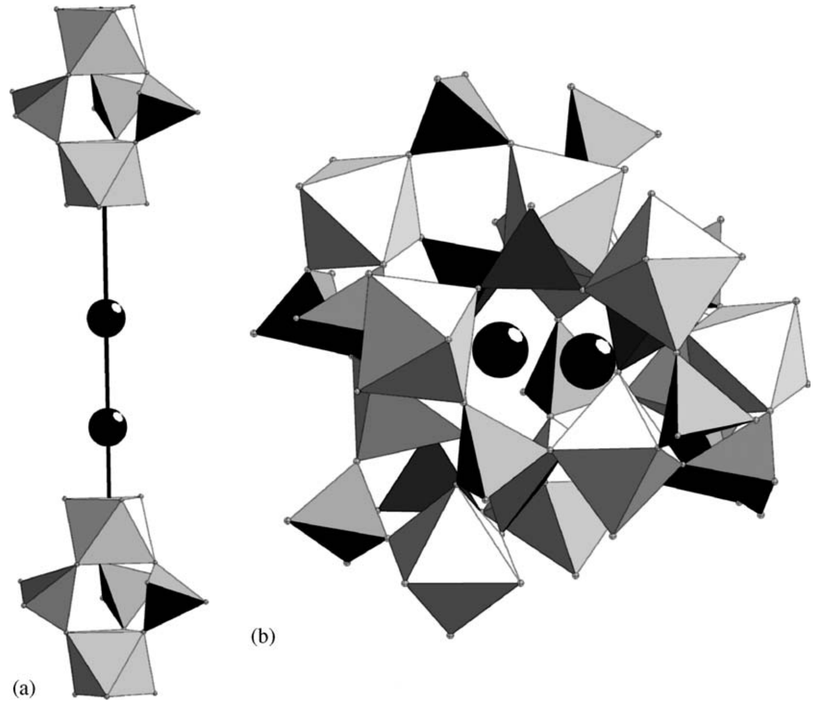

Fig. 1. View of the main fragments: (a) {[Me1O$_6$]–[PO$_4$]$_3$–[Me2O$_6$]–K1–K2} sequence along the [111] direction; (b) big cationic cavity with two potassium ions inside it (big black circles are potassium atoms).

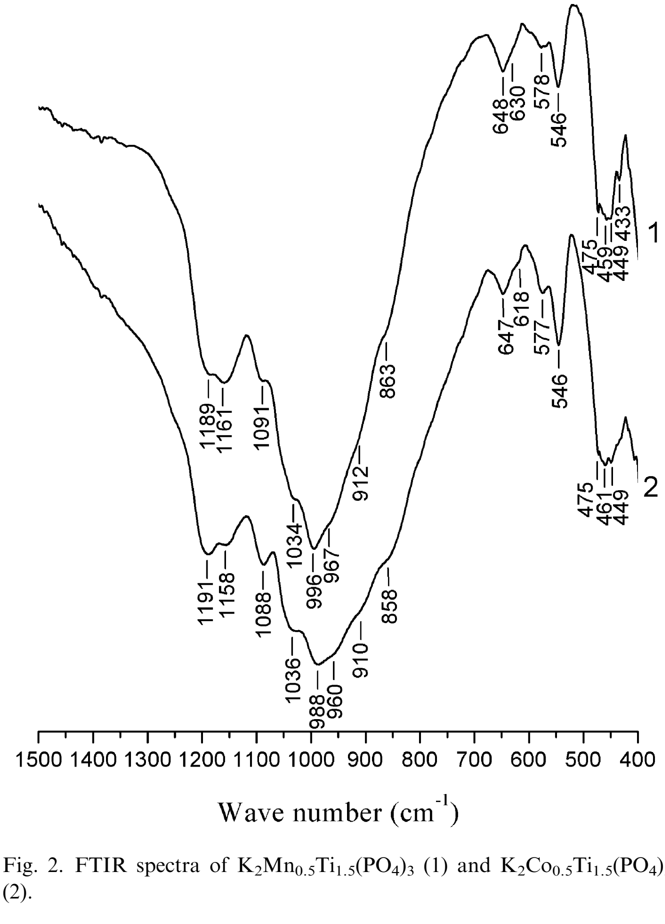

Fig. 2. FTIR spectra of $K_2Mn_{0.5}Ti_{1.5}(PO_4)_3$ (1) and $K_2Co_{0.5}Ti_{1.5}(PO_4)_3$ (2).

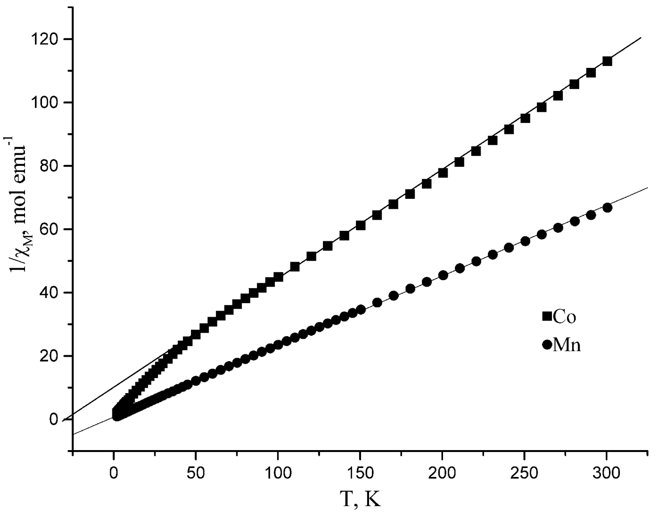

Fig. 3. Thermal variation of reciprocal molar magnetic susceptibility of $K_2Mn_{0.5}Ti_{1.5}(PO_4)_3$ (●) and $K_2Co_{0.5}Ti_{1.5}(PO_4)_3$ (■).

behavior at a full studied temperature range, $\chi = C/(T-\Theta)$, but $K_2Co_{0.5}Ti_{1.5}(PO_4)_3$ displays a Curie–Weiss law behavior at temperature above 50 K. The deviation of the reciprocal molar magnetic susceptibility from the Curie–Weiss law under 50 K for $K_2Co_{0.5}Ti_{1.5}(PO_4)_3$ can be explained by the existence of the weak ferromagnetic interactions. Such a behavior can be connected with the effect of the molecular field and realization of exchange interactions. The interactions are possible because the nearest distances are 4.631(1) and 4.956(1) Å between two cobalt atoms which are interlinked by the bridging orthophosphate groups. The Weiss temperature and Curie constant for $K_2Mn_{0.5}Ti_{1.5}(PO_4)_3$ are $\Theta = -3.24$ K and $C = 4.49$ emu K mol^{-1}, for $K_2Co_{0.5}Ti_{1.5}(PO_4)_3$ are $\Theta = -31.49$ K and $C = 2.96$ emu K mol^{-1} per two formula unit (1 Mn (Co) atom). Effective magnetic moment per Mn center is 6.01 μ_B which is in agreement with the spin only value (5.92 μ_B) of high-spin Mn(II). The corresponding g-value is 2.03 for the manganese compound. For $K_2Co_{0.5}Ti_{1.5}(PO_4)_3$, the effective magnetic moment per Co center of 4.61 μ_B differs a lot from the theoretical spin value (3.87 μ_B) for d^7 shell. The calculated g-value is 2.38 for cobalt phosphate. The experimental value of effective magnetic moment and g factor for $K_2Co_{0.5}Ti_{1.5}(PO_4)_3$ is normal for Co(II) compounds and indicate the presence of the high orbital contribution [17]. As the structure investigation shows the octahedral environment of the paramagnetic atoms have small trigonal distortion which have effect on the μ_{eff} value (Fig. 3).

Acknowledgments

The authors thank Professor Igor O. Fritsky at the Physical Chemistry Department of Taras Shevchenko National University, Kiev, for performing magnetic measurements.

References

[1] R. Masse, A. Durif, J.C. Guitel, I. Tordjman, Bull. Soc. Fr. Miner. Cristallogr. 95 (1972) 47.
[2] A. Leclaire, A. Benmoussa, M.M. Borel, A. Grandin, B. Raveau, J. Solid State Chem. 78 (1989) 227.
[3] E.S. Lunezheva, B. Maximov, O.K. Mel'nikov, L.A. Muradyan, Kristallografiya 34 (1989) 611.
[4] I.V. Zatovsky, N.S. Slobodyanik, D.A. Stratiychuk, K.V. Domasevitch, J. Sieler, E.B. Rusanov, Z. Naturforsch. B 55 (2000) 291.
[5] N.S. Slobodyanik, N.V. Stus, P.G. Nagornyi, A.A. Kapshuk, Russ. J. Inorg. Chem. 36 (1991) 2772.
[6] H. Wulff, U. Guth, B. Loescher, Powder Diffraction 7 (1992) 103.
[7] A.I. Orlova, I.G. Trubach, V.S. Kurazhkovskaya, P. Pertierra, M.A. Salvado, S. Garcia-Granda, S.A. Khainakov, J.R. Garcia, J. Solid State Chem. 173 (2003) 314.
[8] J. Isasi, A. Daidouh, Solid State Ion. 133 (2000) 303.
[9] S.T. Norberg, Acta Crystallogr. B 58 (2002) 743.
[10] E.R. Losilla, S. Bruque, M.A.G. Aranda, L. Moreno-Real, E. Morin, M. Quarton, Solid State Ion. 112 (1998) 53.
[11] T. Droβ, R. Glaum, Acta Crystallogr. E 60 (2004) 58.
[12] V.A. Kopilevitch, L.N. Schegrov, A.F. Gafarova, N.H. Beckmetova, 1988, SU 1535821 A1 USSR.
[13] G.M. Sheldrick, SHELXS86, in: G.M. Sheldrick, C. Kruger, R. Goddard (Eds.), Crystallographic Computing, vol. 3, Oxford University Press, Oxford, 1985, p. 175.
[14] G.M. Sheldrick, SHELXL97. Program for crystal structure refinement, University of Göttingen, Germany, 1997.
[15] A. Zemann, J. Zemann, Acta Crystallogr. 10 (1957) 409.
[16] G. Berthet, J.C. Joubert, E.F. Bertaut, Z. Kristallogr. (A) 136 (1972) 98.
[17] R.L. Carlin, Magnetochemistry, Springer, Berlin, Heidelberg, 1989.